Transducin β-like protein 1 controls multiple oncogenic networks in diffuse large B-cell lymphoma

Youssef Youssef,[1] Vrajesh Karkhanis,[1] Wing Keung Chan,[1] Frankie Jeney,[1] Alessandro Canella,[1] Xiaoli Zhang,[2] Shelby Sloan,[1] Alexander Prouty,[1] JoBeth Helmig-Mason,[1] Liudmyla Tsyba,[1] Walter Hanel,[1] Xuguang Zheng,[1] Pu Zhang,[3] Ji-Hyun Chung,[1] David M. Lucas,[1] Zachary Kauffman,[1] Karilyn Larkin,[1] Anne M. Strohecker,[4,5] Hatice G. Ozer,[6] Rosa Lapalombella,[1] Hui Zhou,[7] Zijun Y. Xu-Monette,[8] Ken H. Young,[8] Ruolan Han,[9] Elmar Nurmemmedov,[10] Gerard Nuovo,[11] Kami Maddocks,[1] John C. Byrd,[1] Robert A. Baiocchi,[1] and Lapo Alinari[1]

[1]Department of Internal Medicine, Division of Hematology, The Ohio State University, Columbus, OH, USA; [2]Center for Biostatistics, Department of Biomedical Informatics, The Ohio State University, Columbus, OH, USA; [3]Division of Pharmaceutics and Pharmaceutical Chemistry, College of Pharmacy, The Ohio State University, Columbus, OH, USA; [4]Department of Cancer Biology and Genetics, The Ohio State University Columbus, OH, USA; [5]Department of Surgery, Division of Surgical Oncology, The Ohio State University Columbus, OH, USA; [6]Department of Biomedical Informatics, The Ohio State University, Columbus, OH, USA; [7]Department of Lymphoma & Hematology, The Affiliated Tumor Hospital of Xiangya Medical School, Central South University, Changsha, Hunan, China. [8]Department of Pathology, Division of Hematopathology, Duke University, Durham, NC, USA; [9]Iterion Therapeutics, Huston, TX, USA; [10]Department of Translational Neurosciences and Neurotherapeutics, John Wayne Cancer Institute, Providence Saint John's Health Center, Santa Monica, CA, USA and [11]Discovery Life Sciences, Powell, OH, USA

 doi:10.3324/haematol.2020.268235

Received: July 27, 2020.

Accepted: September 10, 2020.

Pre-published: September 14, 2020.

Correspondence: *LAPO ALINARI* - lapo.alinari@osumc.edu

Supplementary methods

Cell lines and Primary samples

DLBCL cell lines were grown in standard RPMI-1640 medium supplemented with 10% FBS, 1 mM sodium pyruvate and 1% Penicillin-Streptomycin and routinely confirmed to be Mycoplasma negative (MycoAlert Detection Kit, Lonza).

Primary DLBCL cells were isolated using CD19 magnetic beads and cultured according to standard methods. Patient characteristics in Supplemental Tables 1 and 2. Normal B-, T- and NK-cells of peripheral blood obtained from healthy volunteers were isolated using positive selection magnetic beads (Miltenyi Biotech). Purity of the isolated immune cells was determined by FACS analysis using immune cell subset specific markers. For activating the lymphocytes: B-cell and T-cells were treated with 3.2uM CpG and anti-CD3/CD28 respectively and harvested after 24 hours (doxorubicin was used as positive control for B-cells); NK-cells were treated with IL-2/IL-12/18 and harvested after 15 hours following standard methods.

For germinal center B-cells, total mononuclear cells were isolated from pediatric tonsils as described in[1] without performing any further selection. Cells were then stained with the following antibodies: CD10-PE, CD19-FITC, CD56-APC, CD3-APC, and CD14-PerCP (BD Biosciences) according to the manufacture protocol. CD14-CD3-CD56-CD19+CD10+ cells were then sorted to ≥97% purity with a FACSAriaII sorter (BD Biosciences).

Reagents

Tegavivint was provided by Iterion Therapeutics. MG132, cycloheximide and chloroquine were all purchased from Sigma. Rapamycin and doxorubin were purchased from Selleckchem. Doxycycline was purchased from Tocris.

Tissue microarray (TMA) and Immunohistochemistry (IHC)

For IHC on human samples, hematoxylin-eosin stained slides from each of the 83 cases of DLBCL were reviewed, and TMA was constructed from tumor cell-rich areas. The 83 DLBCL cases were previously reported by Visco C et al. and classified into ABC and GCB based on integrated gene expression profiling and immunohistochemical studies.[2]

IHC studies for a variety of markers using a streptavidin-biotin complex technique were performed on 4-µm TMA sections in all cases. The markers assessed included: CD30, CD10, Bcl-6, GCET1, MUM1, FOXP1, BCL2, MYC, p53, p21 and Ki-67. A cut-off value for each marker was established from analysis of receiver-operating characteristic curves to achieve maximum specificity and sensitivity as described previously. Immunohistochemistry for TBL1 and CD10 (for germinal center identification within normal tonsils) was performed on formalin-fixed paraffin-embedded tissues using an anti-TBL1 antibody (abcam, ab24548) and anti-CD10 antibody (Ventana, 790-4506) according to the manufacturer's instructions. Enzo Life Sciences HRP-conjugated secondary antibody was used for detection. Tissue underwent antigen retrieval in 10mM citrate buffer (pH 9.0) at 95˚C for 30 minutes. TBL1 and CD10 co-expression analysis and quantification was performed with the Nuance Multispectral Imaging System and Fast Red (TBL1: red), and DAB (CD10: brown) with yellow indicating co-expression (Nuance software using the co-localization tool).[3]

TBL1 protein expression was recorded in 5% increments as the percentage of positive lymphoma cells. Tonsillar epithelium and a breast ductal carcinoma tissue biopsy were used as positive controls. Immune cells in the background were used as negative control. After TBL1 staining, patients were dichotomized based on the median percentage of TBL1 positive cells: GCB-DLBCL cases with ≥50% and ABC-DLBCL cases with ≥55% of TBL1 positive cells were defined as high expressors, the remaining patients were defined as low expressors. For samples obtained from the human cell line xenograft model (Riva), all tissues were fixed by immersion in 10% neutral buffered formalin, processed by routine methods and embedded in paraffin. Six µM-thick sections were stained with hematoxylin and eosin on a Leica ST5020 Multistainer (Leica Biosystems, Buffalo Grove, IL) by the

histology laboratory of the Comparative Pathology and Mouse Phenotyping Shared Resource. A board-certified veterinary anatomic pathologist assessed the brain sections under bright-field microscopy (Nikon Ci-L microscope, Nikon Instruments, Melville, NY; representative photomicrographs taken using an Olympus SC180 digital camera, B & B Microscopes Limited, Pittsburg, PA).

Gene knock-down using shRNA and CRISPR-Cas9 systems

Lentiviral particles were produced by transient transfection of 10×10^6 Lenti-X 293T cells (Takara Bio USA Inc.) with 15 µg of vector DNA along with the packaging constructs psPAX (15 µg), and pVSG (3 µg) using Lipofectamine 2000 (Thermo Fisher Scientific). Virus containing supernatants were collected at 72 hr after transfection, and used to infect DLBCL cell lines using spinoculation. Briefly, the cells were mixed with the indicated lentiviral particles at the MOI of no more than 10 and centrifuged at 3900 rpm at 32°C for 90 min. The cells were recovered, and either sorted (GFP+) or incubated at 37°C for 48 hours in puromycin (1ug/mL) to select the stable clones. Three days after selection, the cells were withdrawn with the puromycin selection for 2 days before downstream experiments were performed. The successful knock-down were confirmed by RT-PCR with gene-specific probes/primers in each experiment.

shRNA from Sigma catalogue number for each gene: β-CATENIN: TRCN0000314921, TRCN0000314991; TBL1: TRCN0000299525. CAND1: TRCN000000346. TBL1X Human shRNA Plasmid Kit, CAT#: TL316751 from OriGene Technologies (Rockville, MD).

sgRNA sequences for TBL1 knock-down: TBL1X: Guide 1 targeting exon 2: 5'-TCCCAAACGTGAAAGCCGAG-3'. Guide 2 targeting exon 3 Oligo1 5'-AGACGCCGTGATGCCCGACG-3'. Guide 3 targeting exon 5 Oligo1 5'-CTTTGTTACTCGGGACGTCA-3'

Immunoblot and co-immunoprecipitation assay

Cell were treated with either vehicle control or the indicated concentration of tegavivint at the indicated time points, then for whole cell extracts, cells were lysed in RIPA buffer [10 mM Tris-HCl (pH 7.4), 150 mM NaCl, 1% Triton X-100, 0.1% SDS and 1% sodium deoxycholate] containing protease and phosphatase inhibitors (all from Sigma) and cell lysates were clarified by centrifugation. Nuclear and cytosolic extracts were prepared using the NE-PER kit (Pierce) according to the manufacturer's recommendations. Proteins were analysed by immunoblot using standard procedures. To show TBL1, β-CATENIN and SKP1 interaction, preimmune immune, anti-TBL1, anti-β-CATENIN and anti-SKP1 antibodies were crosslinked to the magnetic beads according to the manufacturer's protocol (abcam). Whole cell extracts were incubated with these crosslinked antibodies overnight at 4°C. Beads were collected by centrifugation, washed five times with 0.5 mL of washing buffer [40 mM Tris-HCl (pH 8.0), 180 mM NaCl], and bound proteins were analyzed by western blotting. Western blots were captured by either using an enhanced chemiluminescence substrate for detection of scant HRP (Thermo Fisher Scientific; Ref 32106) or by LI-COR Biosciences Odyssey Infrared Imaging System using IRDye antibodies (Two-color 181 multiplex detection). Protein bands were normalized using LI-COR Image Studio software (Version 5.2). Western blot bands intensity, for each protein, were first calculated (normalized) considering control sample(s) as the reference. Then the calculated values were normalized based on the difference between the loading control (ACTIN or GAPDH). Details on antibodies used are in Supplemental Table 4.

RNA extraction and RT-PCR

Total RNA from DLBCL cells was isolated using TRIzol reagent (Thermo Fisher Scientific) and RNA Clean-Up and Concentration Kit (Cat. 23600) (Norgen Biotek Corp) according to the manufacture protocol. The mRNA levels of target genes were determined by RT-PCR using predesigned Taqman gene expression assay accordingly to the manufacturer's instruction (ABI Biosystems, Thermo

Scientific). The assays were run on Viia 7 real-time PCR system (ABI Biosystems) and the data was analyzed by ΔCT calculation relative to the reference gene GAPDH. Details on specific primers and probes are in Supplemental Table 5.

Chromatin-immunoprecipitation (ChIP)-Sequencing and ChIP-PCR

For Chip-Seq assays, cell pellets were snap frozen and shipped on dry ice to Active Motif where subsequent steps were performed according to previously published pipeline.[4] TBL1 ChIP reactions were performed using 30 µg of DLBCL cell lines chromatin and 8 µl of TBL1 antibody (abcam, ab24548). Illumina sequencing libraries were prepared from the ChIP and Input DNAs by the standard consecutive enzymatic steps of end-polishing, dA-addition, and adaptor ligation. After a final PCR amplification step, the resulting DNA libraries were quantified and sequenced on Illumina's NextSeq 500 (75 nt reads, single end). Raw sequence reads (75bp single end) were aligned to human reference genome (hg19) using bwa version 0.7.12.[5] Normalized (reads per million) bigwig files were generated using bamCoverage function of deepTools.[5] Heatmaps depicting genome-wide enrichment of the ChIP signal around transcription start site were generated using computeMatrix and plotHeatmap functions of deepTools.[6]

For ChIP-PCR, cross-linked chromatin was prepared from Pfeiffer, Riva and OCI-Ly3 cell lines treated with either vehicle control or biologically relevant concentration of tegavivint for 12 hours. After sonication, cross-linked chromatin was digested with micrococcal nuclease (1 unit/ml) at 37^{o}C for 20 min before adding 200 µL of stop buffer (100 mM Tris-HCl [pH 8.6], 0.45% SDS, 2.5% Triton X-100, 5 mM EDTA [pH 8.0], and protease inhibitors). Chromatin was analyzed by agarose gel electrophoresis to ensure that DNA fragment sizes did not exceed 500 bp, and ChIP assays were carried out essentially as described previously.[7] To amplify DNA sequences of *MYC*, pre-immune and immune antibodies raised against TBL1 (abcam, ab24548), and β-CATENIN (CST; mAb#8814), after extensive washing, nucleoprotein complexes were eluted in 200 µl of elution buffer (50 mM Tris-HCl [pH 8.0],

10 mM EDTA, 1% SDS), and cross-links were reversed by incubating samples at 65^{o}C for 12 hr. Immunoprecipitated DNA was purified by phenol and chloroform extraction, and resuspended in 40 µl of TE buffer (10 mM Tris-Hcl [pH 8.0], 1 mM EDTA). mRNA promoter sequences were amplified using gene-specific primers and locked nucleic acid probes from the Human Universal ProbeLibrary Set (Millipore Sigma). The following primers and probes were used in this study: *MYC* (forward: 5'-GAAATTGGGAACTCCGTGTG-3', reverse: 5'-CTAGGGCGAGAGGGAGGTT-3'; probe 53) and *BIRC5* (forward: 5'-AAGGAGGAGTTTGCCCTGAG-3', reverse: 5'-GGGCCACTACCGTGATAAGA-3'; probe 24).

Confocal microscopy

LC3 tandem reporter (pCDH-CMV-mC-G-LC3B-P was a gift from Kazuhiro Oka (Addgene plasmid # 124974). Accumulation and co-localization of GFP and mCherry fluorescence signals from the GFP–mCherry–LC3 positive B-cell NHL cell lines were examined by laser scanning confocal microscopy. After treatment with the indicated reagents, cells were fixed with 4% paraformaldehyde for 10 minutes at 37°C and then washed with PBS (pH 7.4), and then cytospun on the glass slides. Nuclei were stained with 4′,6-diamidino-2-phenylindole (DAPI) containing mount medium (abcam, ab104139) for 5 minutes at room temperature and then coversliped for confocal microscopy observation. Fluorescence of GFP (green), mCherry (red) and their colocalization (yellow) were analyzed by Olympus Filter FV1000 Laser Scanning Confocal Imaging Systems and IMARIS microscopy image analysis software. At least 100 cells were counted in control and each treatment group.

Proximity Ligation Assay (PLA)

The tegavivint-treated Riva and Pfeiffer cell lines cells were fixed with 4% paraformaldehyde for 10 minutes at 37°C. They were permeabilized with 0.1% Triton-X-100 for 15 minutes at 37°C, washed in PBS and blocked in Duolink Blocking buffer for 30 min at room temperature. Primary antibodies were

diluted in Duolink Antibody Diluent and incubated overnight at 4 °C. Where appropriate, cells were counterstained using Anti-IgG (CST#3900S and CST#5415S), mouse anti-TBL1 (Sigma; SAB1411330), rabbit anti-β-CATENIN (Cell Signalling Technology; 2677), rabbit anti-CUL1 (Sigma: SAB1411513), and mouse anti-CAND1 (Sigma: SAB1405164) primary antibodies overnight. The cells were washed for 20 min in a large volume of PBS with 1% BSA, followed by addition of the appropriate Duolink secondary antibodies. Cells were incubated for 1 h at 37 °C, after which cells were washed in TBST with 0.5% Tween-20 for 10 min. Ligation and amplification steps of the PLA were performed using the Duolink in situ Detection Reagents red kit (Sigma) according to the manufacturer's instructions. Following the PLA, Nuclei were stained with 4′,6-diamidino-2-phenylindole (DAPI) containing mount medium (abcam, ab104139) for 5 minutes at room temperature and then coversliped for confocal microscopy observation. PLA signal was analyzed by using Olympus Filter FV1000 Laser Scanning Confocal Imaging Systems. PLA spots were counted in cell lines using IMARIS software. PLA scores were determined by normalizing the number of PLA spots counted in each sample to the number of cell counted in the same sample. At least 300 cells were counted for each condition.

Cytotoxicity assay

DLBCL Cell lines and primary DLBCL samples were treated with either vehicle control or the indicated concentration of tegavivint 24 hours, then cells were stained with 5 µl of FITC-Annexin V antibody (BD Bioscience) and 5 µl of propidium iodide solution (BD Biosciences) for 15 min at room temperature in the provided buffer before they were analyzed on a BD LSRFortessa™ flow cytometer. Data were analyzed with Flowjo version 10 software (BD Bioscience).

Transmission Electron Microscopy (TEM)

DLBCL cells were treated as indicated and then fixed for 30 minutes in 2.5% glutaraldehyde in 0.1M phosphate buffer, pH 7.4. Further processing was performed by the OSU Campus Microscopy and Imaging Facility. Images were obtained with a FEI Tecnai G2 Spirit TEM.

Animal studies

All animals were monitored daily for signs of tumor burden, including hind limb paralysis, respiratory distress, weight loss, ruffled coat, and distended abdomen. Body weight was measured weekly for the first 3 weeks and then daily. Animals were sacrificed when these symptoms were observed and subjected to histopathologic evaluation to confirm the presence of DLBCL. The primary endpoint of these studies was survival defined as the time from engraftment to the development of the defined clinical criteria leading to removal from the study. NSG mice were purchased from Jackson.

Supplemental Table 1: Patients' characteristics of the DLBCL patient samples (*n*=8).

Patient no.	Age/Sex	DLBCL subtype	Stage at diagnosis	Source of tumor cells	Previous therapy
1	62/M	ABC, double expressor	IVA	Peripheral blood	Yes
2	70/F	GCB, with t(8;14)	IVB	Peripheral blood	No
3	62/M	GCB, with t(8;14)	IVB	Peripheral blood	Yes
4	55/F	ABC	IIIA	LN	No
5	67/M	GCB-DH	IVA	LN	No
6	48/M	DLBCL-NOS, DE, HIV	IVB	LN	Yes
7	59/M	DLBCL-NOS	IVB	BM	No
8	68/F	GCB	IVA	Peripheral blood	Yes

Supplemental Table 2. Patients' characteristics of the 83 DLBCL cases included in Figure 1, D and E.

Patients (*n*=83)	Female (Yes: 1)	B-symptoms (Yes: 1)	Front-line chemo response (R-CHOP)	ABC (Yes: 1)	Percentage of TBL1 positive DLBCL cells	OS (months)	OS status (0=alive; 1=dead)	PFS (months)	PFS status (1= relapsed /refractory)
1	1	0	PR	0	70	13.25	1	13.25	1
2	0	0	CR	0	80	44.35	0	44.35	0
3	1	0	PD	1	90	3.58	1	3.58	1
4	0	1	PR	1	80	11.57	1	11.57	1
5	1	0	PD	0	85	38.6	0	38.6	0
6	0	0	SD	0	5	39.16	0	39.16	0
7	1	1	CR	0	50	36.1	0	36.1	0
8	1	1	CR	0	20	32.25	0	32.25	0
9	1	1	CR	1	5	27.95	0	27.95	0
10	1	0	CR	1	40	29.19	0	29.19	0
11	1	1	CR	0	10	25.58	0	25.58	0
12	0	0	CR	0	70	22.78	0	22.78	0
13	0	1	CR	0	55	16.83	0	16.83	0
14	1	0	CR	0	50	20.91	0	20.91	0
15	0	0	SD	0	65	46.68	0	46.68	0
16	1	1	PR	1	75	3.72	1	3.72	1
17	1	0	CR	0	65	50.63	0	43.89	1
18	0	1	CR	1	75	6.74	1	6.74	1
19	0	1	CR	1	55	57.04	0	57.04	0
20	1	1	CR	0	15	50.4	0	50.4	0
21	1	0	CR	1	35	36.89	0	36.89	0
22	0	0	CR	1	85	15.25	1	15.25	1
23	0	0	CR	0	35	53.95	0	53.95	0
24	0	0	CR	0	30	61.87	0	61.87	0
25	0	1	CR	0	50	53.69	0	53.69	0
26	0	0	CR	1	10	38.89	1	38.89	1
27	1	1	CR	1	65	74.5	0	74.5	0
28	0	1	CR	0	5	73.78	0	73.78	0
29	1	0	CR	1	75	75.06	0	75.06	0
30	0	0	CR	1	40	36.16	0	36.16	0
31	0	0	CR	1	45	66.31	1	66.31	1
32	0	0	CR	1	30	78.12	0	78.12	0
33	0	0	PD	0	65	1.94	1	1.22	1
34	1	1	CR	0	30	70.98	0	70.98	0
35	1	0	CR	1	10	79.76	0	41.06	1
36	0	0	PR	0	60	8.32	1	8.32	1
37	0	1	CR	1	65	84.3	0	11.47	1
38	1	0	CR	0	40	84.2	0	84.2	0
39	0	0	CR	1	60	68.75	0	68.75	0

40	0	1	PD	0	70	9.37	1	9.37	1
41	0	1	CR	0	10	88.54	0	88.54	0
42	0	1	CR	0	55	91.43	0	91.43	0
43	0	0	CR	0	80	91.86	0	91.86	0
44	0	0	CR	0	50	63.81	1	63.81	1
45	1	0	CR	0	10	92.84	0	92.84	0
46	0	0	CR	0	20	105.9	0	105.9	0
47	1	1	CR	0	55	36.53	1	35.7	1
48	1	.	PR	1	30	113.03	0	23.18	1
49	1	1	CR	0	70	10.19	1	10.19	1
50	1	0	CR	0	40	102.67	0	102.67	0
51	0	0	CR	1	30	98.99	1	98.99	1
52	0	0	CR	0	40	25.35	1	25.35	1
53	0	0	CR	1	60	99.42	0	53.52	1
54	0	1	CR	0	80	56.45	1	56.45	1
55	0	0	CR	0	80	91.96	0	91.96	0
56	1	1	CR	1	30	91.53	0	91.53	0
57	1	0	CR	0	15	85.48	0	85.48	0
58	1	0	CR	1	35	88.14	0	88.14	0
59	0	0	CR	0	20	86.53	0	86.53	0
60	1	0	CR	0	80	91.53	0	7.36	1
61	0	0	CR	0	65	16.87	1	16.87	1
62	1	1	CR	1	35	77.42	0	77.42	0
63	1	0	CR	0	40	72.92	0	72.92	0
64	0	0	CR	1	15	72.59	0	72.59	0
65	0	0	CR	1	25	67.86	0	67.86	0
66	1	0	CR	0	60	66.97	0	66.97	0
67	0	0	CR	1	70	55.76	0	55.76	0
68	0	1	CR	0	25	53.95	0	53.95	0
69	0	0	CR	1	50	59.15	0	59.15	0
70	0	1	PD	0	75	5.85	1	4.87	1
71	0	0	CR	1	70	86.47	0	86.47	0
72	1	0	CR	1	60	125.16	0	125.16	0
73	0	0	CR	1	15	66.38	0	66.38	0
74	1	0	CR	1	70	21.27	1	8.42	1
75	0	0	CR	1	60	58.62	1	53.59	1
76	1	1	CR	0	20	98.53	0	98.53	0
77	0	1	PR	0	35	93.14	1	93.14	1
78	0	1	PR	1	55	10.82	1	10.65	1
79	0	1	PD	1	80	5.06	1	5.06	1
80	1	0	CR	1	35	25.84	1	25.84	1
81	0	0	CR	0	5	124.04	0	124.04	0
82	1	0	CR	0	65	43.96	1	26.17	1
83	1	1	PD	1	85	0.69	1	0.69	1

Supplemental Table 3. International Prognostic Index (IPI) of the 83 DLBCL cases included in Figure 1, D and E.

Patients (*n*=83)	Age>60	stage III-IV (Yes=1)	Serum LDH (High:1)	>1 extranodal sites (yes=1)	ECOG>1 (yes=1)	IPI>2 final
1	0	0	1	0	0	0
2	0	1	1	0	0	0
3	1	1	1	0	0	1
4	0	1	1	1	0	1
5	0	1	1	0	0	0
6	0	0	1	0	1	0
7	0	1	1	0	0	0
8	0	0	.	0	.	0
9	1	0	1	0	0	0
10	1	0	1	0	0	0
11	0	1	1	0	0	0
12	0	0	1	0	0	0
13	1	0	1	0	0	0
14	0	1	1	0	1	1
15	0	1	1	0	0	0
16	1	1	1	0	1	1
17	0	0	0	0	0	0
18	0	1	1	1	1	1
19	0	1	0	1	0	0
20	1	0	0	0	0	0
21	0	1	1	1	0	1
22	1	0	0	0	0	0
23	0	0	0	0	0	0
24	0	0	0	0	0	0
25	0	1	1	0	0	0
26	1	0	1	0	0	0
27	1	0	1	0	0	0
28	1	1	0	0	0	0
29	1	0	0	0	0	0
30	1	0	1	1	0	1
31	1	0	1	0	0	0
32	1	1	1	0	0	1
33	1	1	1	0	0	1
34	0	1	1	0	0	0
35	1	0	0	0	0	0
36	1	1	1	0	0	1
37	0	0	1	0	0	0
38	1	0	0	0	0	0
39	0	0	1	0	0	0
40	1	0	1	0	0	0

41	0	1	1	0	0	0
42	1	0	0	0	0	0
43	0	0	1	0	0	0
44	1	0	0	0	0	0
45	0	0	0	0	0	0
46	1	0	0	0	0	0
47	1	0	1	0	0	0
48	0	.	.	.	.	.
49	1	1	1	1	0	1
50	1	0	0	0	0	0
51	1	0	0	0	0	0
52	1	0	0	0	0	0
53	1	1	1	0	1	1
54	1	1	1	0	1	1
55	1	1	0	1	0	1
56	1	1	0	0	1	1
57	0	0	0	0	0	0
58	0	1	1	0	0	0
59	1	1	0	0	0	0
60	0	1	1	1	0	1
61	1	0	0	0	0	0
62	0	0	0	0	0	0
63	1	0	0	0	0	0
64	1	1	0	1	0	1
65	0	1	1	0	0	0
66	1	0	0	0	1	0
67	1	0	0	0	0	0
68	0	1	1	1	1	1
69	1	0	0	0	0	0
70	0	1	1	1	1	1
71	1	0	0	0	0	0
72	0	1	1	0	0	0
73	1	1	0	0	1	1
74	1	0	1	0	0	0
75	0	1	1	0	0	0
76	0	0	1	0	0	0
77	0	1	0	0	1	0
78	1	1	1	1	0	1
79	0	1	1	1	1	1
80	1	1	1	0	0	1
81	0	0	1	0	0	0
82	1	1	0	0	0	0
83	1	1	1	1	0	1

Supplemental Table 4. Immunoblot Antibodies.

Western blot antibodies	**Source**
TBL1X	GeneTex (GTX107736), abcam (ab24548) and Invitrogen (MA5-24874).
ACTIN	Santa Cruz Biotechnology (sc-47778)
Non-phospho active β-CATENIN	CST#2745
MYC	CST#18583
Phospho MYC (Ser62)	CST#13748
GAPDH	CST#5174 and Invitrogen (39-8600)
β-CATENIN	CST#8480
microtubule-associated protein 1 light chain 3 (LC3A/B)	CST#12741
BECLIN-1	CST#4122
CUL1	abcam (ab11047)
Phospho MYC (thr58)	Abcam (ab28842)
CAND1	CST#8759 and Sigma Aldrich (SAB1405164)
PLK1	CST #4513 and abcam (ab17056)
SKP1	CST #12248
Histon H3	CST #4499
SURVIVIN	CST #2808

Supplemental Table 5. RT-PCR primers.

Gene name	**PCR primer**
MYC	assay ID Hs00153408_m1
BIRC5	assay ID Hs00153353_m1
PLK1	assay ID Hs00983227_m1
Endogenous control GAPDH	assay ID Hs02758991_g1
WISP1	assay ID Hs00180245_m1
AXIN2	assay ID Hs00610344_m1
CTNNB1	assay ID Hs00355045_m1
TBL1X	assay ID Hs00959540_m1
CAND1	assay ID Hs00218384_m1
BECN1	Assay ID Hs01007018_m1

Supplemental Figures

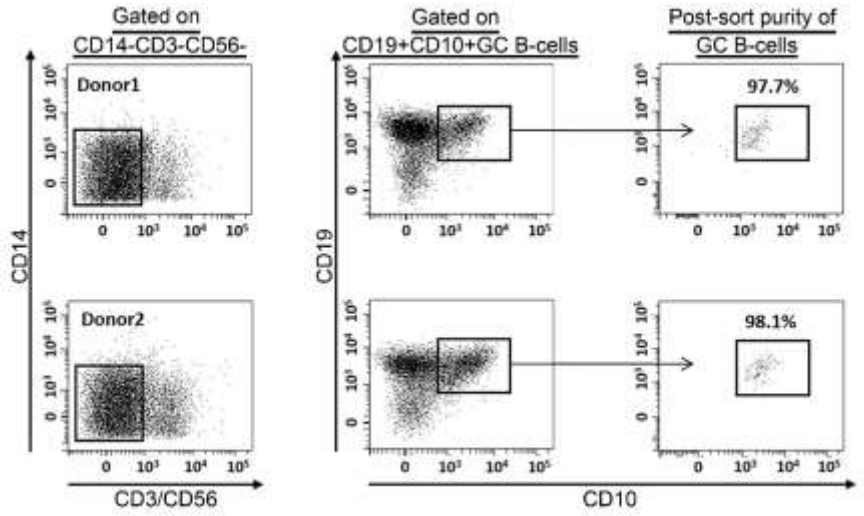

S. Figure 1. Sorting strategy for normal GC B-cells isolation from pediatric tonsils. Dot plots of flow cytometry analysis showing sorting strategy and post-sort purity check of the germinal center (GC) B-cells used in Figure 1A. Mononuclear cells were isolated from two different pediatric tonsils (*n*=2) and then stained before sorting with anti-CD10, anti-CD19, anti-CD14, anti-CD56 and anti-CD3. $CD19^{+}CD10^{+}$ gated germinal center B-cells were sorted after excluding Monocytes (CD14+) , T-cells (CD3+) and NK-cells (CD56+). Numbers above the black boxes represent post-sort purity of the sorted GC B-cells from each donor.

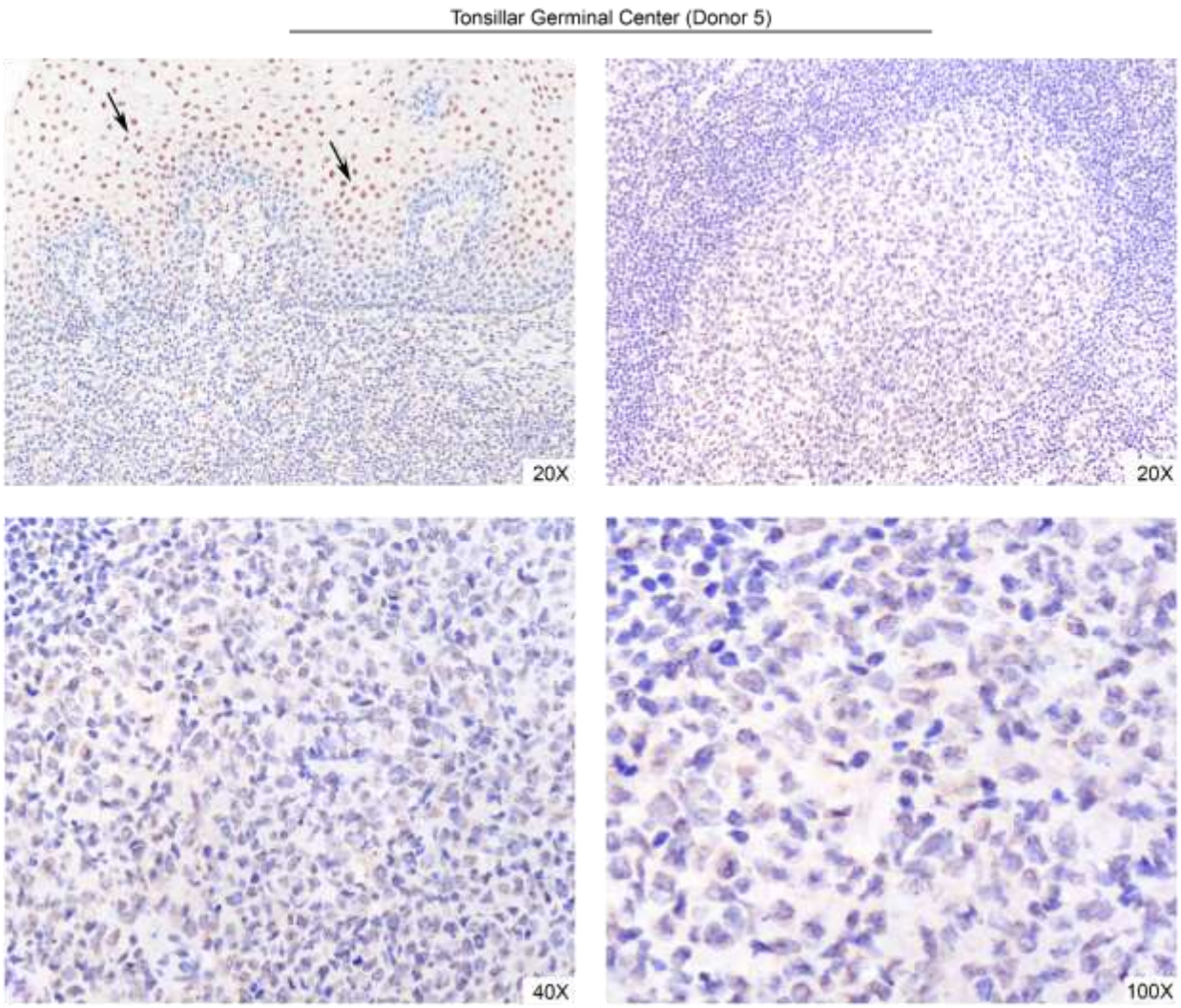

S. Figure 2. TBL1 is expressed at low level in reactive germinal center. Representative images of TBL1 immunohistochemical staining of reactive germinal center from pediatric tonsil (donor 5) (at 20x, 40x and 100x) showing weak positivity for TBL1 (brown). Tonsillar epithelium (black arrows) served as an internal positive control.

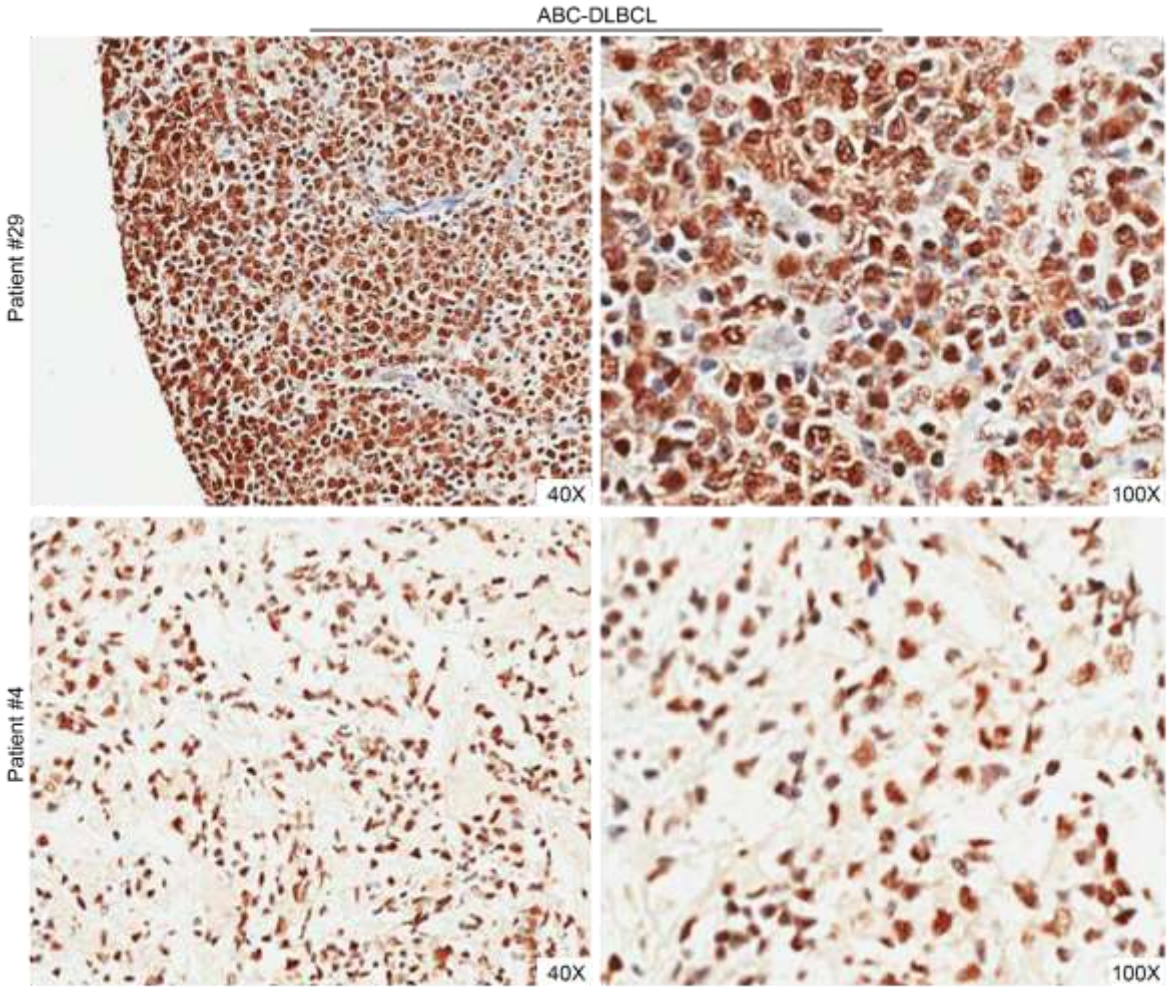

S. Figure 3. TBL1 expression in *de novo* ABC-DLBCL. Representative images of TBL1 immunohistochemical (IHC) staining of lymph nodes involved by ABC-DLBCL (at 40x and 100x) showing diffuse, strong nuclear and cytoplasmic positivity for TBL1.

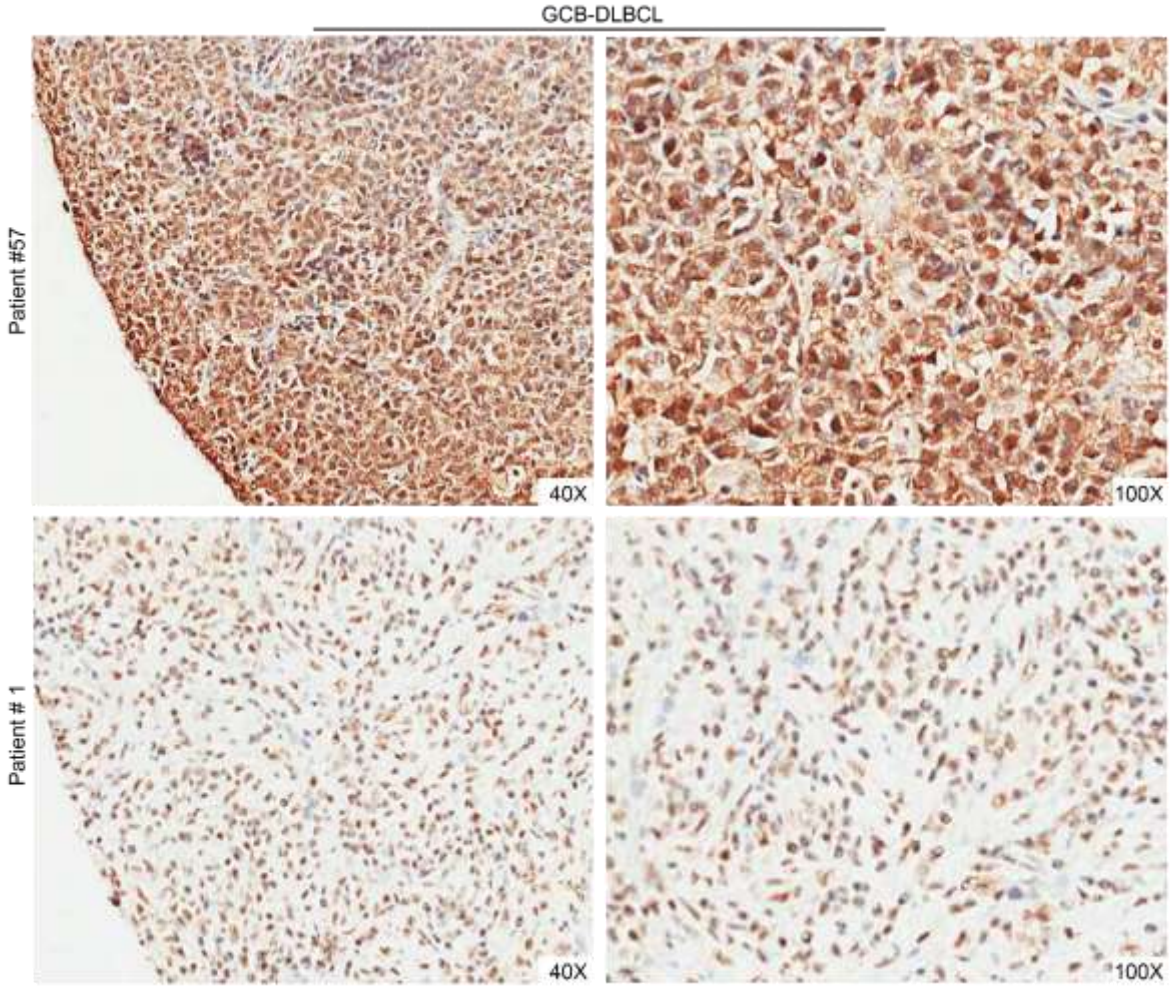

S. Figure 4. TBL1 expression in *de novo* GCB-DLBCL. Representative images of TBL1 immunohistochemical (IHC) staining of lymph nodes involved by GCB-DLBCL (at 40x and 100x) showing diffuse, strong nuclear and cytoplasmic positivity for TBL1.

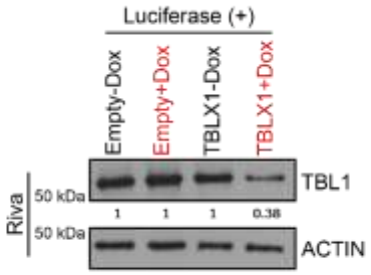

S. Figure 5. Immunoblot validating efficient TBL1 knock-down in the luciferase positive CRISPR-Cas9 engineered Riva cells prior to engraftment into NSG mice (*in vivo* experiment described in Figure 2B). Empty vector was used as control (*n*=1). ACTIN was used as a loading control. Numbers below the immunoblots reflect normalized value of quantified protein bands relative to the controls.

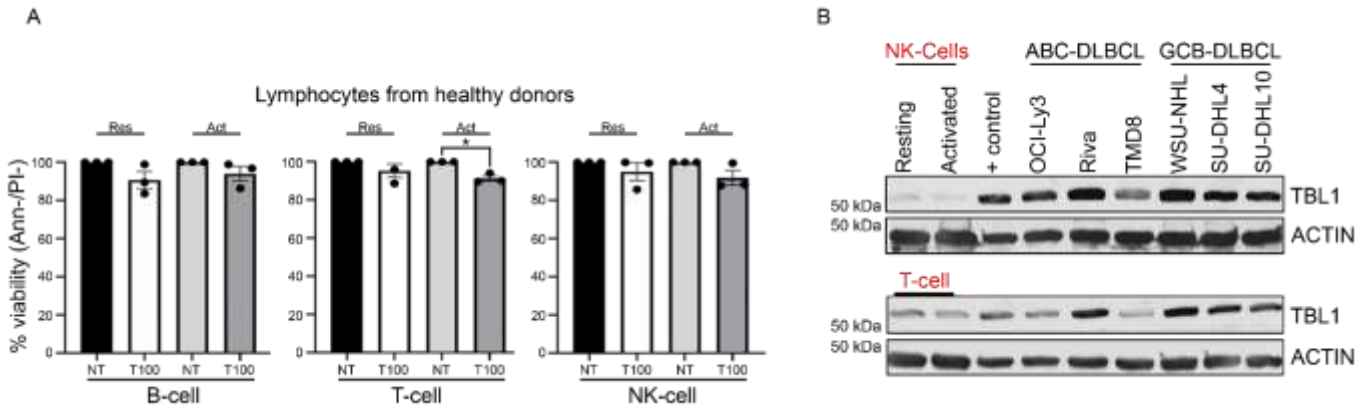

S. Figure 6. Tegavivint is minimally cytotoxic against normal immune cell subsets. (A) Cytotoxicity assay in normal resting (Rest) and activated (Act) lymphocytes (B-cells, T-cells and NK-cells) from 3 healthy donors treated with the indicated concentration of tegavivint (T) in nM. Viability was determined by annexin/propidium iodide (PI) staining and flow cytometry at 24 hours. The graph shows normalized percentage of live cells (ann-/PI- cells) relative to the untreated control (NT). *n*=3, data represent means ± SEM. **p*<0.05 by linear mixed effects models with testing the interaction between treatment and activation status. **(B)** Immunoblot showing abundant TBL1 expression in the indicated DLBCL cell lines compared to normal resting and activated NK and T lymphocytes. ACTIN was used as a loading control (*n*=1).

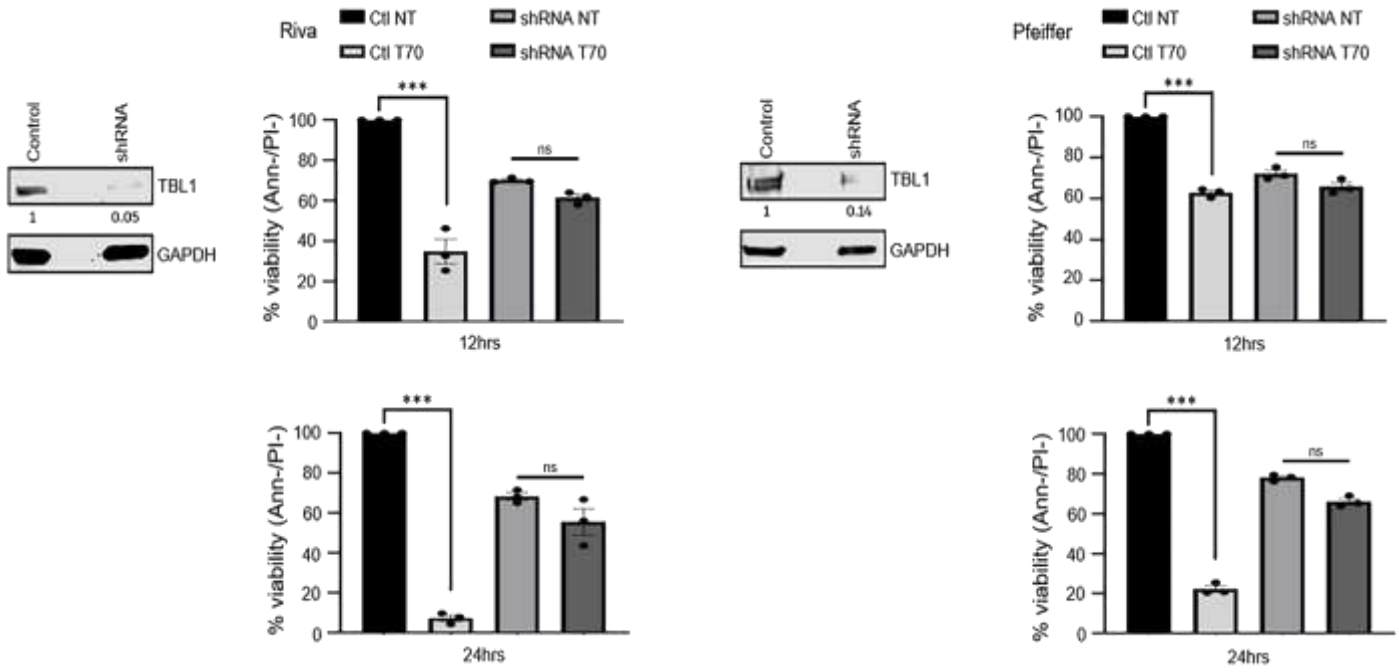

S. Figure 7. Tegavivint selective cytotoxicity: TBL1 was knocked-down in the indicated DLBCL cell lines using a TBL1-specific shRNA construct. Scramble was used as control. Following verification of efficient TBL1 knock-down via immunoblot (72 hours after transduction), DLBCL cells were incubated with 70nM of tegavivint (T70) for 12 and 24 hours. Viability was assessed by annexin/propidium iodide (PI) staining and flow cytometry. Graphs show normalized percentage of live cells (ann-/PI- cells) relative to the untreated scramble control (NT) from three separate experiments. ns: $p>0.05$, *$p<0.05$, **$p<0.005$ by paired t-test. For immunoblot, GAPDH or actin were used as loading control. Numbers below the immunoblot reflect normalized value of quantified protein bands relative to control (1).

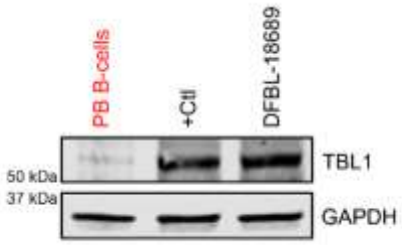

S. Figure 8. TBL1 is abundantly expressed in purified DFBL-18689 cells: Immunoblot showing abundant TBL1 expression in whole cell lysates from DFBL-18689 cells compared to normal human peripheral blood (PB) B-cells. Mantle cell lymphoma cell line (Jeko) was used as positive control (+ Ctl). GAPDH was used as a loading control.

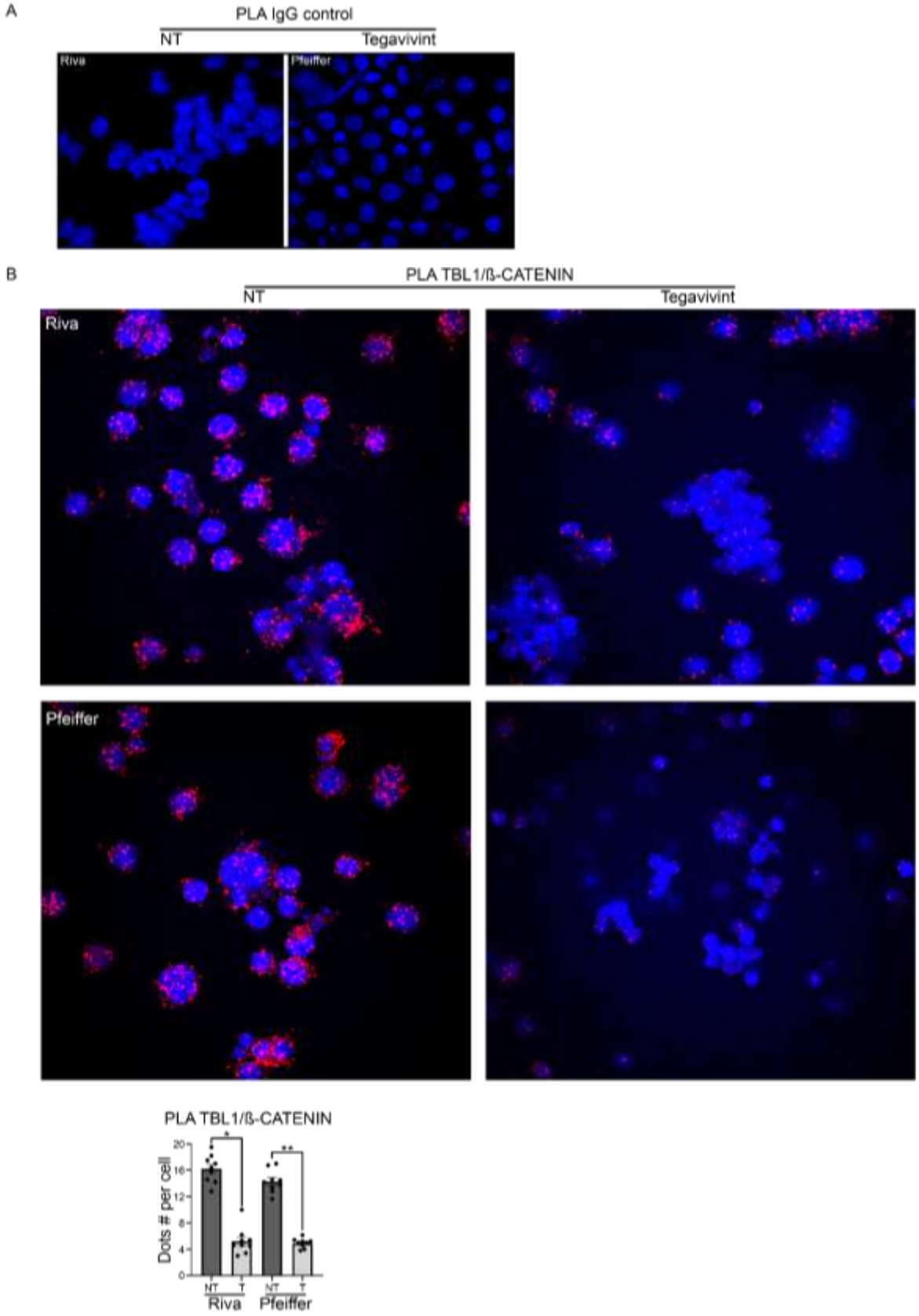

S. Figure 9. TBL1/β-CATENIN loss of proximity upon treatment with tegavivint: (A) Confocal images of PLA (60x) showing the negative IgG control in the indicated DLBCL cells lines. Blue indicates cell nuclei (Dapi) (*n*= 3). **(B)** Confocal images of PLA (100x) using anti-TBL1 and β-CATENIN antibodies in the indicated DLBCL cells lines after treatment with either DMSO control (NT)

or tegavivint (T) (70nM) for 12 hours. Red indicates PLA signal, blue indicates cell nuclei (Dapi) (n= 3). Graph represents the mean value of PLA signal from no less than 300 cells. *p<0.05, **p<0.005 by paired t-test.

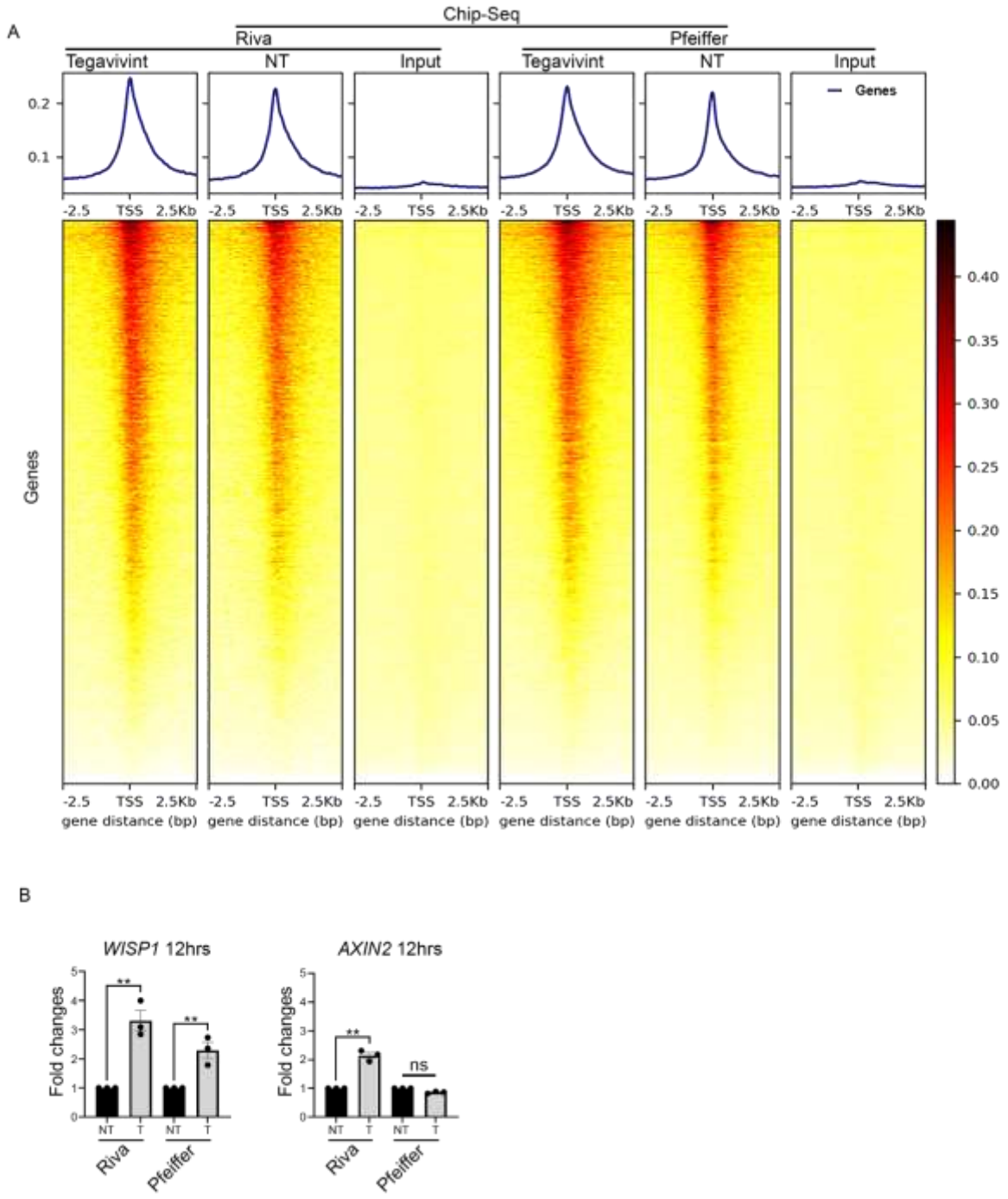

S. Figure 10. Genome-wide TBL1 promoter occupancy is unffected by tegavivint treatment. (A) Representative heat map of ChIP-seq read densities for TBL1 in the indicated DLBCL cell lines after treatment with either DMSO control (NT) or tegavivint (T, 70nM) ranked by decreasing combined occupancy signals centered ± 2.5 kb relative to transcriptional start site (TSS) of transcriptionally active peak regions (*n*= 3). **(B)** qRT-PCR showing the mRNA fold changes of the indicated genes after treating the indicated DLBCL cell lines with tegavivint (T) for 12 hours relative to the untreated control (NT). *n*=3, data represent means ± SEM. ns: *p*>0.05, ***p*<0.005 by paired t-test.

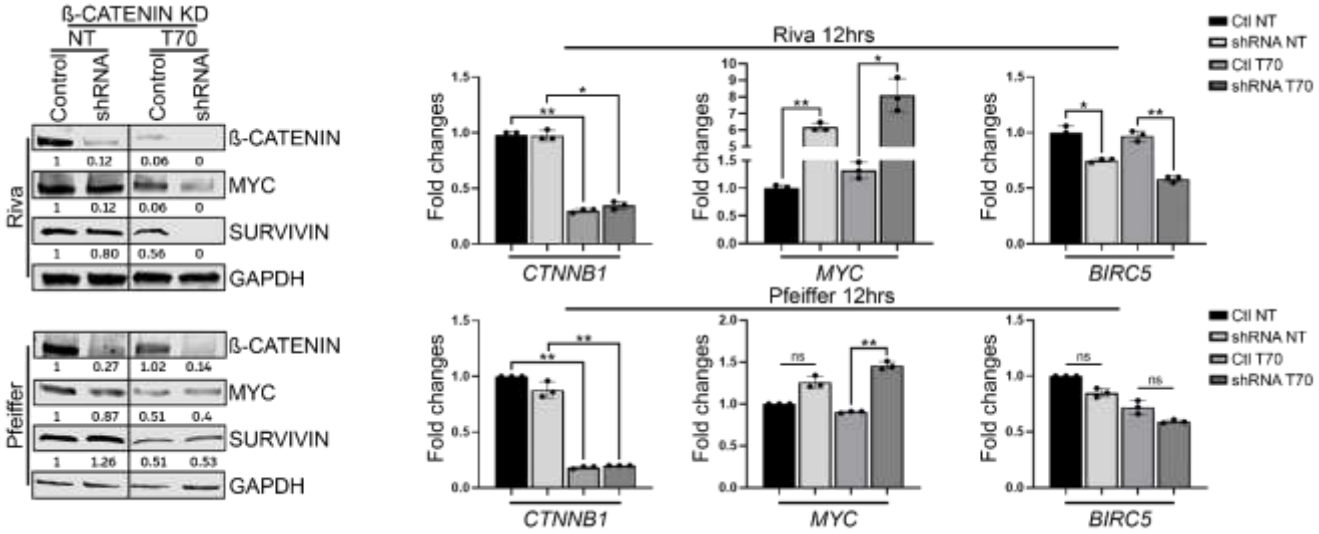

S. Figure 11. TBL-1 mediated/β-CATENIN independent effects on known Wnt/β-CATENIN **targets:** β-CATENIN was knocked-down (KD) in the indicated DLBCL cell lines using a β-CATENIN specific shRNA construct. Scramble was used as control. 72 hours after transduction, cells were treated with 70nM of tegavivint (T70) for 12 hours. β-CATENIN, MYC and SURVIVIN protein expression levels and mRNA fold changes were assessed by immunoblot (left) and qRT-PCR (right), respectively. Immunoblot represent one gel. GAPDH was used as loading control. Numbers below the immunoblot images reflect normalized value of quantified protein bands relative to the controls. n=3, data represent means ± SEM. ns: $p>0.05$, *$p<0.05$, **$p<0.005$, ***$p<0.0005$ by linear mixed effects models incdluing testing the interaction between shRNA and treatment condition.

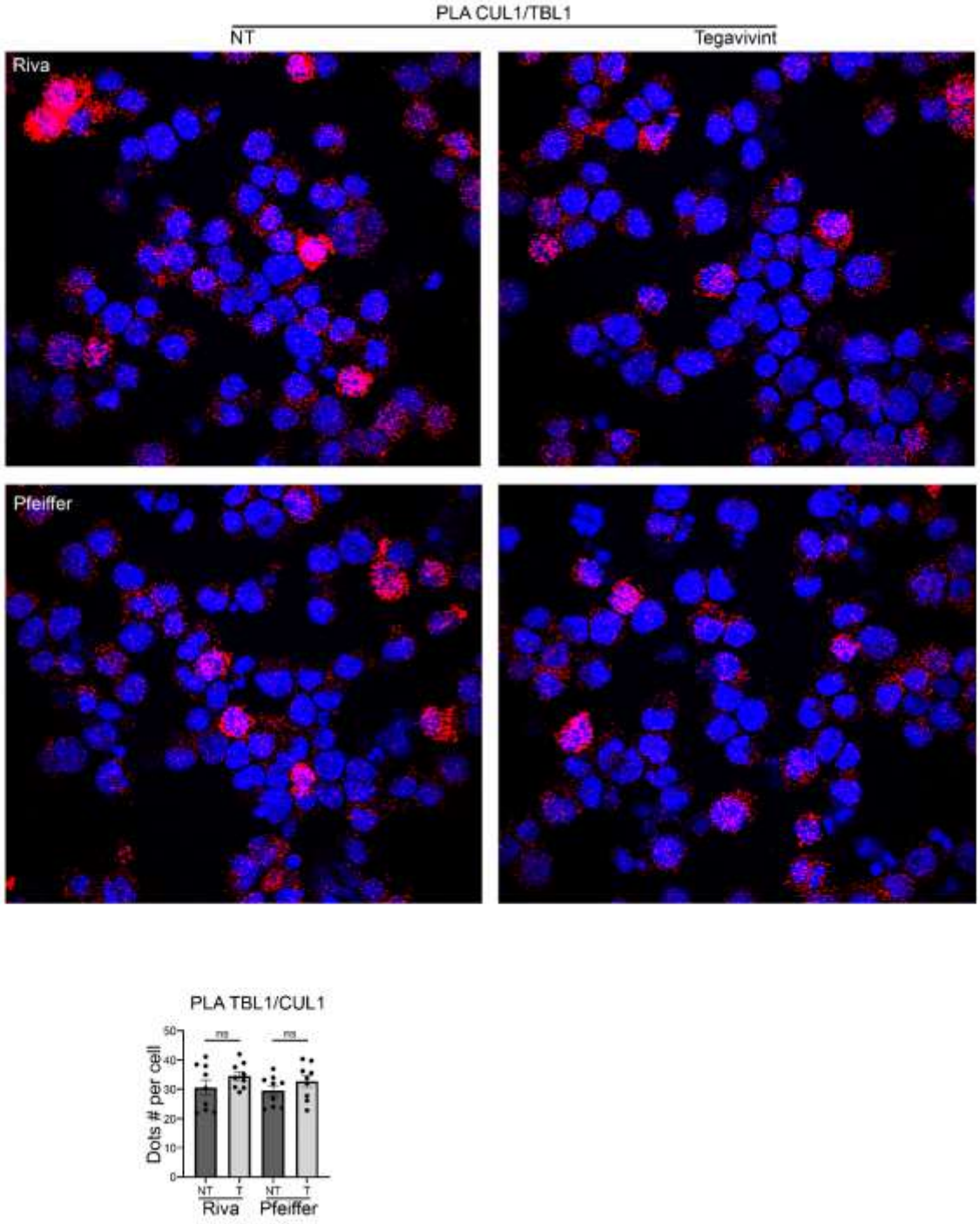

S. Figure 12. Tegavivint does not affect CUL1/TBL1 proximity. Confocal images of PLA (100x) (red) using anti-CUL1 and TBL1 antibodies in the indicated DLBCL cells lines treated with either DMSO control (NT) or tegavivint (T) (70nM) for 12 hours. Red indicates PLA signal, blue indicates cell nuclei (Dapi) (*n*=3). Graph represents the mean value of PLA signal from no less than 300 cells. ns: *p*>0.05 by paired t-test.

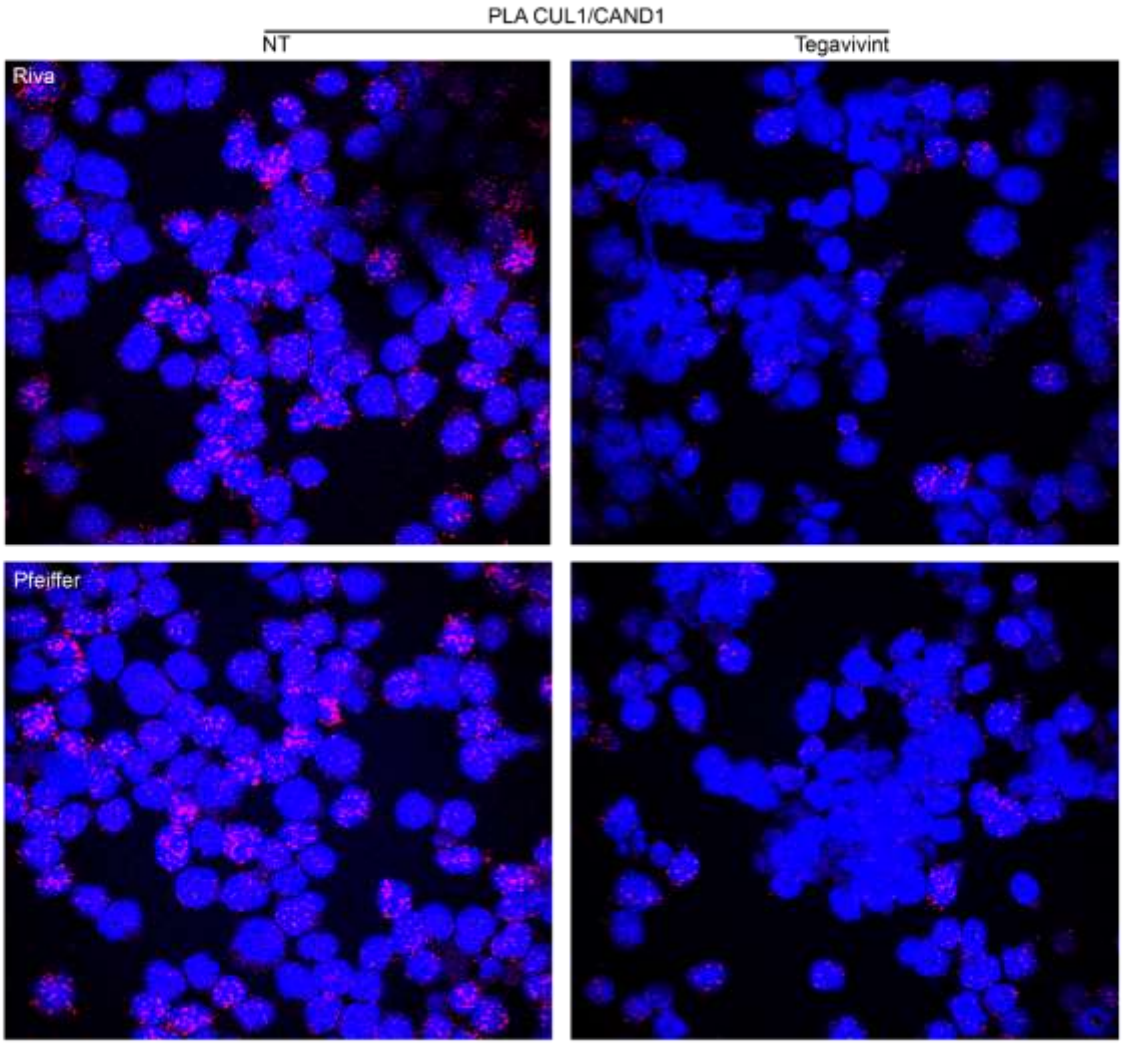

S. Figure 13. Loss of CUL1/CAND1 proximity upon treatment with tegavivint. Confocal images of PLA (100x) (red) using anti-CUL1 and anti-CAND1 antibodies in the indicated DLBCL cells lines treated with either DMSO control (NT) or tegavivint (T) (70nM) for 12 hours. Red indicates PLA signal, blue indicates cell nuclei (Dapi) (*n*=3).

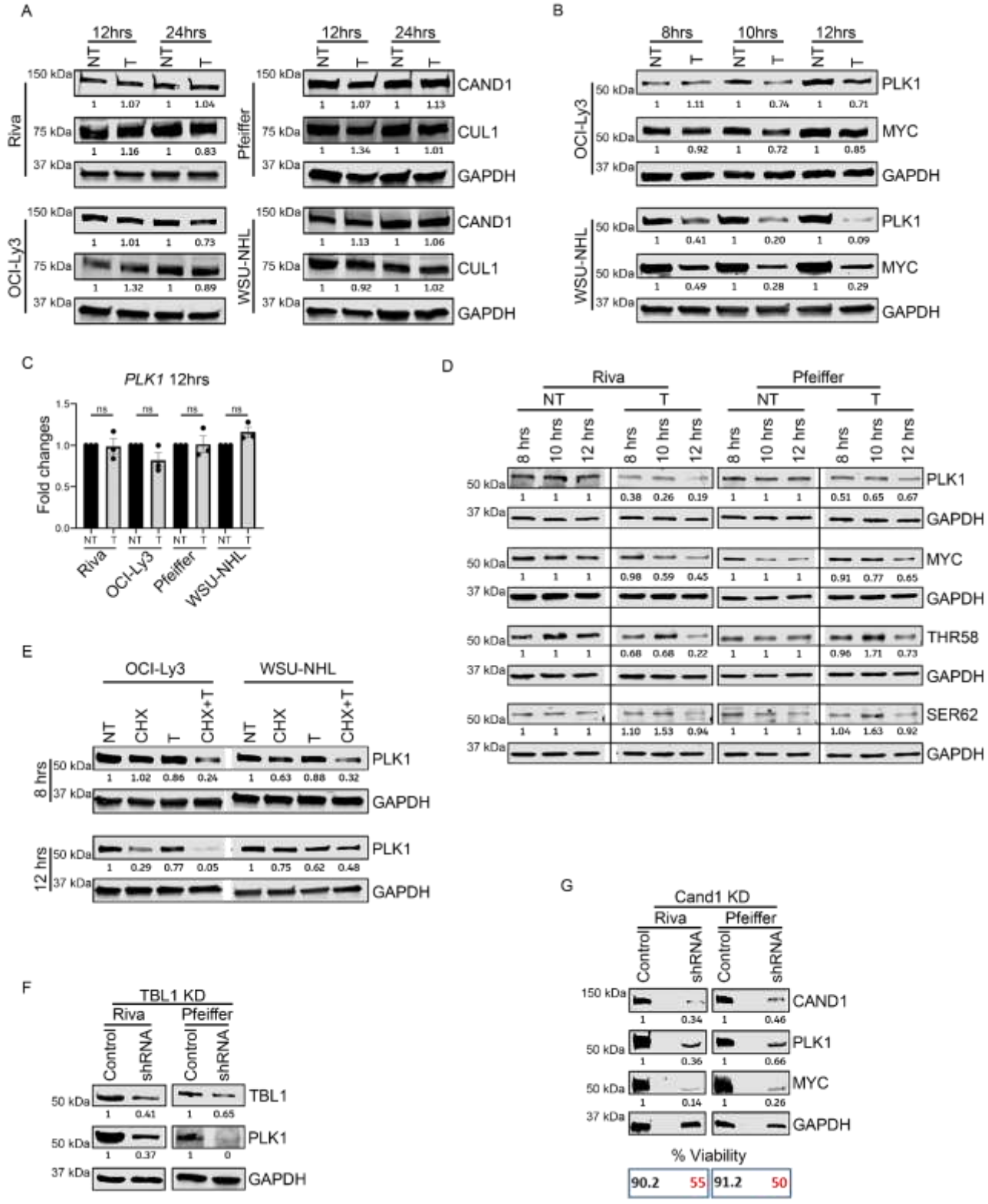

S. Figure 14. TBL1 is part of a SCF complex that modulates the stability of critical oncoproteins. (A) Immunoblot showing CAND1 and CUL1 expression in the indicated DLBCL cell lines after treatment with either DMSO control (NT) or tegavivint (T) for 12 and 24 hours (*n*=3). **(B)** Immunoblot showing time course expression of PLK1 in the indicate DLBCL cell lines after treatment with either DMSO control (NT) or tegavivint (T) (*n*=3). **(C)** qRT-PCR showing mRNA fold changes of *PLK1* at 12 hours after treating the indicated DLBCL cell lines with tegavivint (T) relative to the

untreated control (NT). *n*=3, data represent means ± SEM. ns: *p*>0.05 by paired t-test for each cell line. **(D)** Immunoblot showing time course expression of PLK1, MYC, and phosphorylated MYC (Thr58 and Ser62) in the indicated DLBCL cell lines after treatment with either DMSO control (NT) or tegavivint (T) (from the same gel, *n*=3). **(E)** Immunoblot showing PLK1 expression in the indicated DLBCL cell lines after treatment with either DMSO control (NT), cycloheximide (CHX, 70ug/mL), tegavivint (T) or the combination (CHX+T) for 8 and 12 hours (*n*=3). **(F)** Immunoblot showing PLK1 expression after TBL1 knock-down (KD) in the indicated DLBCL cell lines using a TBL1 specific shRNA construct (*n*=3). **(G)** Immunoblot showing MYC and PLK1 expression after CAND1 knock-down (KD) in the indicated DLBCL cell lines using a CAND1 specific shRNA. Numbers in the blue box below the immunoblot indicate percentage of viable DLBCL cells by trypan blue exclusion from one experiment (*n*=1). Numbers below the immunoblot images reflect normalized value of quantified protein bands relative to the controls (1). Tegavivint (T): Riva and Pfeiffer: 70nM, OCI-ly3: 50nM and WSU-NHL: 15nM. MG132: Riva, OCI-Ly3 and WSU-NHL: 0.5uM and Pfeiffer: 0.3uM added 6 hours following tegavivint treatment.

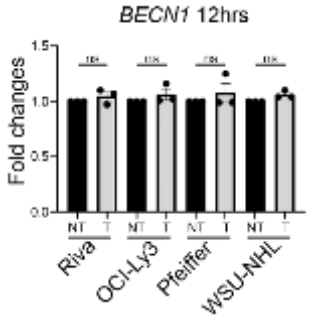

S. Figure 15. Tegavivint does not significantly affect Becn-1 transcript. qRT-PCR showing the mRNA fold changes of *Becn-1* after treating the indicated DLBCL cell lines with tegavivint (T) for 12 hours relative to the untreated control (NT). *n*=3, data represent means ± SEM. ns: *p*>0.05 by paired t-test for each cell line. Tegavivint (T): Riva and Pfeiffer: 70nM, OCI-ly3: 50nM and WSU-NHL: 15nM.

Supplementary References

1. Scoville SD, Keller KA, Cheng S, et al. Rapid column-free enrichment of mononuclear cells from solid tissues. Sci Rep. 2015;5(1):1-6.
2. Visco C, Li Y, Xu-Monette ZY, et al. Comprehensive gene expression profiling and immunohistochemical studies support application of immunophenotypic algorithm for molecular subtype classification in diffuse large B-cell lymphoma: a report from the International DLBCL Rituximab-CHOP Consortium Program Study. Leukemia. 2012;26(9):2103-2113.
3. Fiore C, Bailey D, Conlon N, et al. Utility of multispectral imaging in automated quantitative scoring of immunohistochemistry. J Clin Pathol2012;65(6):496-502.
4. de Almeida Nagata DE, Chiang EY, Jhunjhunwala S, et al. Regulation of tumor-associated myeloid cell activity by CBP/EP300 bromodomain modulation of H3K27 acetylation. Cell Rep 2019;27(1):269-281. e264.
5. Li H, Durbin R. Fast and accurate short read alignment with Burrows–Wheeler transform. bioinformatics. 2009;25(14):1754-1760.
6. Ramírez F, Ryan DP, Grüning B, et al. deepTools2: a next generation web server for deep-sequencing data analysis. Nucleic Acids Res. 2016;44(W1):W160-W165.
7. Pal S, Baiocchi RA, Byrd JC, Grever MR, Jacob ST, Sif S. Low levels of miR-92b/96 induce PRMT5 translation and H3R8/H4R3 methylation in mantle cell lymphoma. EMB J. 2007;26(15):3558-3569.